

Decoding auditory and tactile attention for use in an EEG-based brain-computer interface

Winko W. An^{*}, Hakim Si-Mohammed[‡], Nicholas Huang[§], Hannes Gamper[†], Adrian KC Lee[¶],
Christian Holz[†], David Johnston[†], Mihai Jalobeanu[†], Dimitra Emmanouilidou[†],
Edward Cutrell[†], Andrew Wilson[†], Ivan Tashev[†]

^{*}Carnegie Mellon University, Pittsburgh, PA, USA

[‡]Inria, Rennes, France

[§]Johns Hopkins University, Baltimore, MD, USA

[¶]University of Washington, Seattle, WA, USA

[†]Microsoft Research, Redmond, WA, USA

Abstract—Brain-computer interface (BCI) systems offer a non-verbal and covert way for humans to interact with a machine. They are designed to interpret a user’s brain state that can be translated into action or for other communication purposes. This study investigates the feasibility of developing a hands- and eyes-free BCI system based on auditory and tactile attention. Users were presented with multiple simultaneous streams of auditory or tactile stimuli, and were directed to detect a pattern in one particular stream. We applied a linear classifier to decode the stream-tracking attention from the EEG signal. The results showed that the proposed BCI system could capture attention from most study participants using multisensory inputs, and showed potential in transfer learning across multiple sessions.

Index Terms—Attention, auditory, BCI, EEG, tactile

I. INTRODUCTION

BRAIN-COMPUTER interface (BCI) systems offer a non-verbal and covert way for humans to communicate a control signal to a computer. Among the neuroimaging modalities that are currently available, electroencephalography (EEG) has become the most popular choice for BCI applications due to its noninvasiveness, mobility, and low cost [1]. EEG monitors brain activity through sampling the electrical potential along the scalp at a very high rate. The high temporal resolution of EEG oscillations allows capturing certain neural signatures of a brain state or mental efforts, which can be used to decode users’ intention.

Many successful BCI systems rely on external stimulation, especially with visual stimuli. For example, visual P300 is a well-studied event-related potential (ERP) that is elicited as a response to infrequent events, or “oddballs.” It usually happens around 300 ms after the onset of the event, and could be captured by sensors in the parietal area [1]. Another popular neural signature of visual stimuli is the steady-state visual evoked potential (SSVEP), which is the response in

the visual cortex to a constant-frequency flickering stimulus. These vision-based paradigms have high efficiency for transmitting bits to a computer, which can be quantified by their information transfer rate (ITR). Previous studies yielded an ITR of 20.26 bits/min using P300 [2], or 30.10 bits/min using SSVEP [3].

A major disadvantage of using visual stimuli for BCI is the level of visual attention required to complete the task in the presence of competing stimuli and the fact that it could interfere with competing tasks (e.g., walking, driving) when vision is primarily involved. It also requires correctable vision and voluntary gaze control, making it inaccessible to users with severe visual impairment or locked-in-syndrome. In view of this, previous studies have focused on developing an attention-based BCI system using auditory or tactile stimuli. They used modulated signals with a constant carrier frequency as the input, usually in multiple streams of spatial sound [4] or vibration on fingers [5]. Attention was decoded from auditory steady-state response (ASSR) or steady-state somatosensory evoked potential (SSSEP), where the EEG signal is locked to the modulation frequency of the attended stream. However, these sinusoidal carriers with a constant frequency were perceived by users to be annoying or fatiguing [6]. There were also no behavioral metrics to verify the attentional state of the participants. Separately, another recent work on auditory selective attention revealed that lateralized alpha-band (8–12 Hz) power could be a more effective neural signature than ASSR for use in BCI [7]. This is in line with previous studies that have shown an important role of parietal alpha activity in attention to auditory stimuli [8], [9], even while walking [10].

The current study proposes a user-friendly, attention-based BCI paradigm using auditory and tactile stimuli. A task was embedded in the stimuli, which demanded attentional focus from the participants. The auditory stimuli were spatialized melodies, which sound more pleasant and are easier to attend to than monotones. The tactile stimuli were pulsed vibrations applied to the user’s wrists, so that their hands were freed for other hypothetical concurrent work. Both the melodies and the vibrations were amplitude-modulated, which might induce

^{*‡§} Work done as research intern at Microsoft Research, Redmond

[¶] Work done as consulting researcher at Microsoft Research, Redmond

steady-state responses. Since various neural signatures (e.g., ASSR, SSSEP, lateralized alpha and gamma activity) could be expected from the EEG signal, the multisensory attention was decoded by an individualized linear model with full spectral information (from alpha to gamma band). The model’s ability in transfer learning was also evaluated through recording a subset of participants across multiple sessions.

II. METHOD

A. Participants

Twelve adults (32.2 ± 7.4 years old, 3 female) volunteered to participate in this study. Eleven participants were novel to BCI upon recruitment, among which seven had no experience with EEG experiments. No participants reported known history of neurological disorder or hearing loss.

B. Experiment

Before the experiment started, the participants were asked to sit comfortably in front of a computer, read the instructions from the screen, and familiarized themselves with the stimuli. The experiment consisted of 3 blocks using auditory stimuli, 3 blocks using tactile stimuli, and 3 blocks using both auditory and tactile stimuli simultaneously (mixed). At the beginning of each block, a text message (“audio”, “tactile” or “mixed”) was presented in the center of the screen, indicating the sensory modality about to be stimulated. The order of the blocks was randomized for each participant.

The experiment for audio blocks was adapted from a previous study on auditory selective attention [11]. Two streams of modulated signals were used as stimuli, with one presented to the left ear, and the other to the right ear. The audio signals were delivered through a pair of MaximalPower RHF 617-1N earpieces which transmit sound through acoustic tubes, thus reducing possible electromagnetic interference with the EEG signal. Each stream had multiple standard (S), high-pitched (H) and low-pitched notes (L). Each note contained six harmonics of the fundamental frequency (f_0), making it sound more natural than a single sinusoid. The configurations of the two streams are summarized in Table I. The left stream was formed by 9 repetitions of 400-ms notes, among which the first five were always standard (Fig. 1a). The f_0 of the last four notes determined whether the melodic pattern of the stream was “rising” (\dots -S-H-H-H-H), “falling” (\dots -S-L-L-L-L) or “zig-zag” (\dots -S-H-H-S-S). Similarly, the right stream was formed by 12 repetitions of 300-ms notes, with the first five always being standard. The melodic pattern of this stream could be “rising” (\dots -S-H-H-H-H- \dots), “falling” (\dots -S-L-L-L-L- \dots), or “zig-zag” (\dots -S-H-H-H-S- \dots), depending on the f_0 of the last seven notes. The two streams always started at the same time and were played back simultaneously.

There were 24 trials in each audio block. At the beginning of each trial, a visual cue (VC) was shown on the screen to direct the participant’s attention to the left stream, right stream or neither of the two (Fig. 1c). The cue was replaced by a white fixation dot after 1 second, and two streams of melodies started to play 0.5 second later. The participants were asked to identify

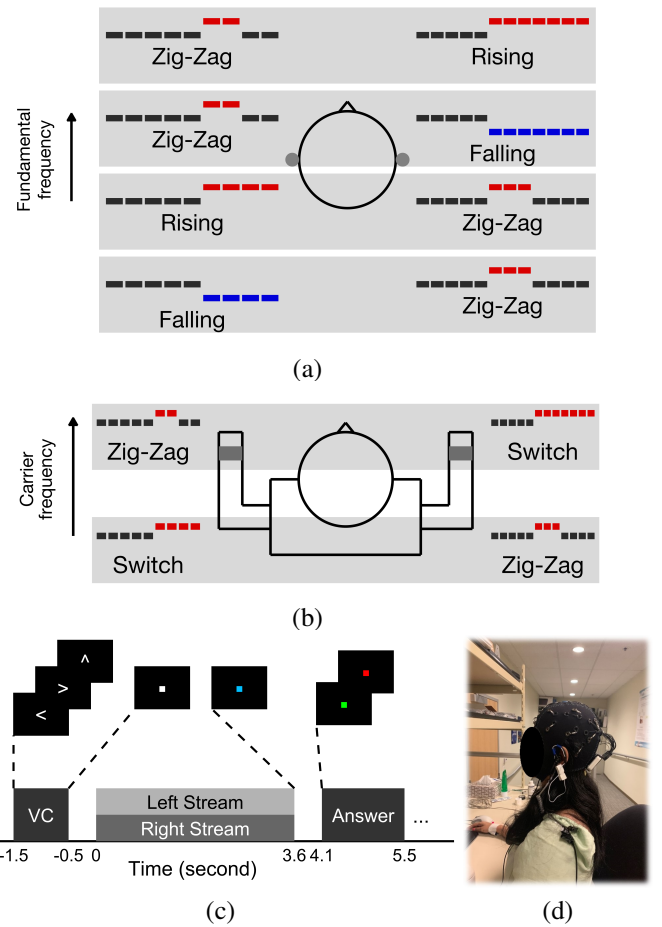


Fig. 1. Illustration of (a) four scenarios of left and right sound streams in an audio block; (b) two scenarios of left and right vibration streams in a tactile block; (c) event sequence in one trial; (d) photograph illustrating the experimental setup.

TABLE I
CONFIGURATIONS OF SOUND STREAMS

Stream	Length (ms)	Modulation frequency (Hz)	Fundamental frequency (Hz)		
			Low	Standard	High
Left	400	37	703	740	777
Right	300	44	396	440	484

the melodic pattern of the attended stream and answer with the keyboard after the fixation dot turned blue. Visual feedback at the end of each trial indicated whether they identified the melodic pattern correctly (green dot) or incorrectly (red dot). The average behavioral performance was shown at the end of each block. The inter-trial interval was set to 2 seconds.

The design of the tactile experiment was analogous to that of the auditory one. The tactile stimuli consisted of two streams of vibration which were applied separately to the left and right wrist of the participant. The streams were rendered through two coin-type loudspeakers (DAEX19CT-4, Dayton Audio) taped to the participant’s wrists (Fig. 1d). Similar to the audio blocks, modulated signals in the form of pulse trains were used for both streams. Their configurations are shown in Table II.

TABLE II
CONFIGURATIONS OF VIBRATION STREAMS

Stream	Length (ms)	Modulation frequency (Hz)	Carrier frequency (Hz)	
			Standard	Oddball
Left	400	27	120	210
Right	300	17	120	210

The modulation and the carrier frequencies were carefully selected through piloting, so that the participants could feel, but not hear the vibration. Unlike in the audio blocks, where there were three types of notes (S, H and L), there were only two types of vibration pulses in tactile blocks, standard (S) and oddball (O). The reason behind this difference is that though most participants could perceive a change in the tactile carrier frequency, they were unable to identify whether it was increasing or decreasing relative to S. Hence, a single oddball condition was the only choice for the tactile experiment. The design of the two spatially separated vibration streams was very similar to that of the sound streams (Fig. 1b). The first five pulses in the left stream were always standard, and the last four could form a “switch” pattern (· · · -S-O-O-O) or a “zig-zag” pattern (· · · -S-O-O-S-S). The first five pulses in the right stream were always standard, and the last seven could form a “switch” (· · · -S-O-O-O-· · ·) or a “zig-zag” (· · · -S-O-O-S-· · ·) pattern. There were 24 trials in each tactile block. In analogy to the audio condition, the participants were asked to identify the vibration pattern in the attended stream and respond with the keyboard.

In multisensory (“mixed”) blocks, the streams of sound and vibration that were used in the audio and the tactile blocks were played concurrently. The melodic pattern and the vibration pattern of the streams on the same side of the participant were matched. For example, a “rising” or “falling” left sound stream was matched to a “switch” left vibration stream; a “zig-zag” right sound stream was matched to a “zig-zag” right vibration stream. Since the notes and pulses on the same side had the same length, when the two streams were played simultaneously, the onset of the frequency change for the two sensory modalities on the same side was synchronized. The task was the same as the one for the audio blocks, where the participants were asked to identify the melodic pattern of the attended stream.

The user interface for all tasks was created in MATLAB. During the experiment, EEG signals were collected using a wireless, gel-based 24-channel system (mBrainTrain Smarting), at a sampling of 500 Hz.

C. EEG processing

The EEG signals were processed using EEGLAB [12] functions and custom MATLAB scripts. The signals were first band-pass filtered by a finite-impulse-response bandpass filter with cut-off frequencies at 0.1 Hz and 50 Hz. After re-referencing to the common average, an adaptive mixture independent component analysis (AMICA) [13] method was used to separate noise and artifact components from the

signals. An automatic EEG artifact detector, ADJUST [14], was then used to select and remove components representing eye blinks and movement. On average, 3.08 ± 1.67 components were removed from each participant.

The continuous EEG data were then segmented into epochs for further analysis. Each epoch contained data within 500 ms before and 3600 ms after the stimulus onset of each trial. The 216 epochs (9 blocks x 24 trials/block) were then divided into 9 conditions depending on their sensory modality (audio/tactile/mixed) and attention type (attend left/attend right/no attention). The EEG data were further cleaned by removing trials with extreme values, which might represent random noise or strong motion artifacts. Trials with peak values beyond three standard deviations from their conditional average were removed from the pool. On average, 21.54 ± 1.62 trials per condition remained for each participant.

D. Feature extraction and classification

A participant-specific linear discriminant analysis (LDA) model was used to decode attention type (left, right or no attention) from single-trial EEG data within each one of the three sensory modalities (audio, tactile or mixed). Spectral information of each epoch, in the form of the magnitude of its Fast Fourier Transform (FFT) coefficients (8 - 50 Hz), was used as the feature to train and test the model. The FFT was calculated using a 3-second sliding window with 90% overlap. Since an epoch (4.1 seconds) was longer than the FFT window length, multiple samples were drawn from each trial, which served well for the purpose of data augmentation. Features of multiple channels were concatenated into a single vector. Its dimensionality was then reduced by principal component analysis (PCA) retaining 99% of the variance.

The accuracy of each 3-way classification was derived from a 10-fold cross-validation (1000 repetition). To prevent information leakage, trials were divided into training and testing sets before data augmentation. The classification of one trial was done by averaging the sample-level posterior probabilities of all testing samples that belonged to that trial, and choosing the one with the highest probability as the decoding output.

E. Feature weight estimation

In order to verify whether the decoding was based on neurologically relevant factors, a post-hoc feature weight estimation was run using neighbourhood components analysis (NCA). It estimated the weight of each feature dimension. The feature before PCA was used for this analysis, and each estimated weight represented the importance of one frequency bin at one particular channel.

F. Cross-session validation

In order to evaluate the transfer learning ability of the proposed BCI system, three participants were invited back to repeat the exact experiment one week after their first attempt. They were chosen based on their decoding score from Session 1 — one with the highest score (participant 72, >70%), one around the average (participant 45, ~60%), and one around the

TABLE III
DECODING ACCURACY AND INFORMATION TRANSFER RATE (ITR)

Modality	Average decoding	Average ITR (bits/min)	Best ITR (bits/min)
Audio	54.18%	1.90	13.69
Tactile	60.87%	3.37	18.27
Mixed	58.02%	2.69	11.57

chance level (participant 78, $\sim 40\%$). Classification was first done using the within-session decoding method as described above, i.e., training and testing an LDA model using the data only from Session 2. A subsequent cross-session decoding was conducted by training a model with data from one session, and having it tested on another. The cross-session decoding result was compared to that of the within-session decoding to evaluate the model’s ability to generalize.

III. RESULTS

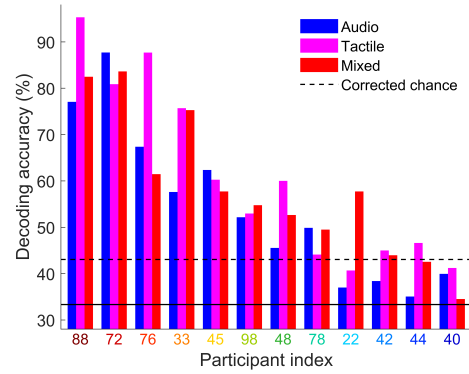
A. Attention decoding

The absolute chance level of a 3-way decoding is 33.33%. However, studies on brain signal classification, like the current one, are generally susceptible to a high chance of false positives due to small sample size. To tackle this problem, Combrisson and Jerbi [15] suggested calculating the chance level as a function of sample size, number of classes, and the desired confidence interval based on a binomial cumulative distribution. Using this method, the significant chance level in this study is corrected to 43.06% ($p=0.05$).

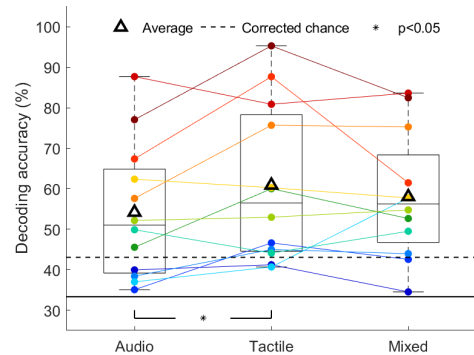
The decoding accuracy of most participants exceeded the corrected chance level, despite the existence of substantial individual differences (Fig. 2a). EEG of 4 participants were not significantly classifiable in at least one sensory modality, while 3 participants’ decoding was over 70% in at least two sensory modalities. The highest decoding accuracy for audio, tactile and mixed conditions were 87.72%, 95.32% and 83.63%, respectively. Their equivalent ITRs are shown in Table III. Within the three types of sensory modalities, tactile conditions had the highest average decoding accuracy (Table III), which is significantly higher than that of audio conditions ($p=0.0348$).

B. Behavioral performance

Most participants could identify the melodic patterns with high accuracy for the audio ($92.53\% \pm 9.10\%$) and the mixed ($93.92\% \pm 7.91\%$) conditions (Fig. 3). Out of the 12 participants, 6 completed the audio or the mixed task with a perfect score. The tactile task appeared to be the most difficult, with a behavioral performance ($65.28\% \pm 16.89\%$) significantly lower than that of the other two sensory modalities ($p < 0.001$). Only one participant completed the tactile task with more than 90% correct. One interesting observation is that the behavioral performance in tactile blocks seemed to divide the participants into two subgroups — one with a performance score above 75% ($n=5$), and one below ($n=7$). The behavioral results of these subgroups in other sensory modalities were not separable.



(a)



(b)

Fig. 2. (a) The decoding accuracy of each participant in the order of high to low average score. (b) The decoding accuracy grouped by sensory modality. Each line represents a participant. The lines and labels are color-coded, where a warmer color denotes a higher average decoding score.

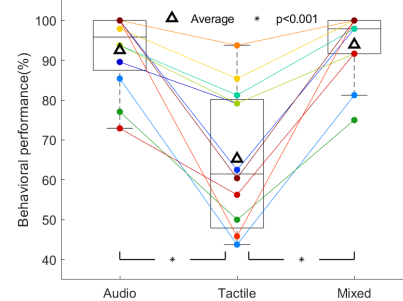


Fig. 3. The behavioral results of all participants performing the pattern identification task in each sensory modality. Each line represents a participant. The lines are color-coded by the participant’s average decoding accuracy (same as in Fig. 2).

C. Behavioral correlate

Despite the fact that the highest decoding score and the worst behavioral performance both happened in tactile blocks, there was no significant correlation between these factors across subjects (Fig 4). Neither a linear nor a quadratic function could fit all the data in tactile blocks with high confidence. However, a subgroup analysis revealed that the

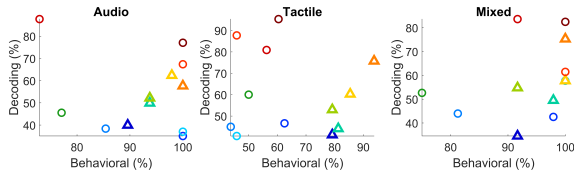


Fig. 4. Correlation between behavioral performance and attention decoding. Each circle or triangle represents a participant whose behavioral performance in tactile blocks was below or above 70%, respectively. The circles and triangles are color-coded by the participant’s average decoding accuracy (same as in Fig. 2).

participants with a high behavioral score in tactile task (>70%) had a linear behavioral correlate with their decoding score in all sensory conditions. This relationship was not seen in the other subgroup with low behavioral scores in tactile task.

D. Feature weight

The estimated feature weights of 4 participants with good decoding scores are shown in Fig. 5. Surprisingly, high weights are not associated with any of the modulation frequencies as in an ASSR/SSSEP feature (dashed lines). Instead, they appear mostly in alpha (8 – 12 Hz) and gamma bands (>30 Hz) in these participants (shaded regions). Topographic maps of maximum feature weights in alpha band reveal dominant patterns in the parietal and occipital channels, especially in decoding tactile attention (Fig. 6). For gamma band feature weights, the dominant patterns reside in the frontal and temporal channels. (Fig. 7).

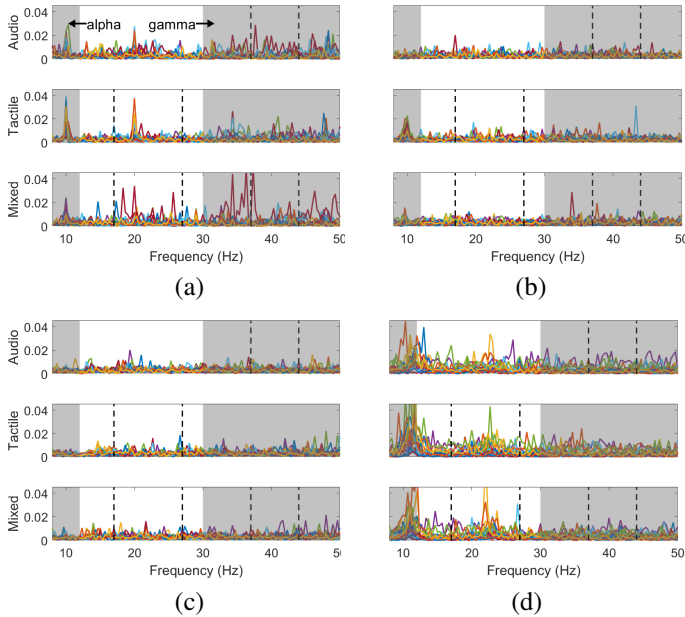


Fig. 5. Estimated feature weights for participant (a) 72 (b) 76 (c) 33 (d) 45. Each trace represents a channel. Y-axis has arbitrary unit. The dashed lines in each panel represent the modulation frequencies of the stimuli used for that particular sensory modality. The shaded regions denote the alpha and the gamma bands

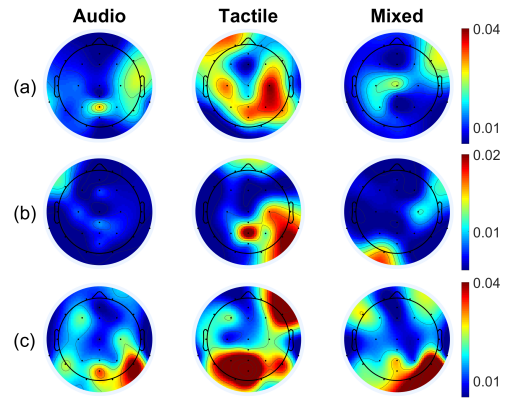


Fig. 6. Topographic maps of maximum feature weights in alpha band for participant (a) 72 (b) 76 (c) 45.

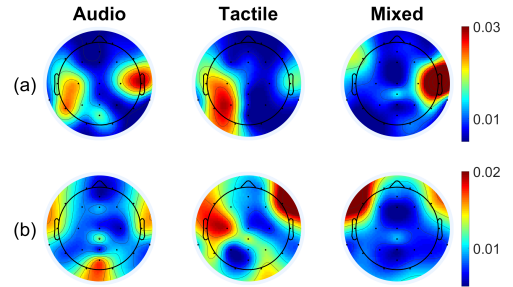


Fig. 7. Topographic maps of maximum feature weights in gamma band for participant (a) 72 (b) 33.

E. Cross-session validation

Three participants were invited to repeat the experiment for cross-session validation. The decoding scores of participant 45 and 78 from Session 2 were in line with their results from Session 1 (Fig. 8). The scores of participant 88 dropped from the first session, but still remained high in all three modalities. Notably, the cross-session validation of all three participants stays in the same range as their within-session decoding.

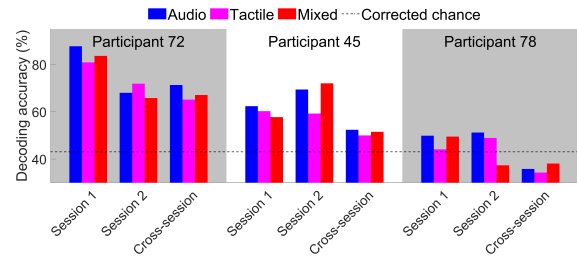


Fig. 8. Decoding result of the cross-session validation analysis

IV. DISCUSSION

A. Transmission efficiency

The efficiency of the proposed BCI system is on par with previous works. The average ITR derived from audio

blocks (1.90 bits/min) was comparable to previous studies on ASSR-based BCIs [6], [16]. The average ITR in tactile blocks outperformed the results of previous BCI designs with vibrotactile actuators attached to the user's thumb (~ 1.19 bits/min, calculated from the reported accuracy) [5], or five fingers (1.2 bits/min) [17]. A recent study reported a higher ITR (4.9 bits/min), but electrical stimulation on four fingers was needed [18]. Promisingly, the highest ITR achieved in the tactile condition was comparable to that of some vision-based BCI systems previously reported [19]. There is great potential in improving the decoding results with the current dataset. For example, the pattern identification task used in this experiment is not dissimilar to detecting oddball events. One possible direction is to combine a P300 feature into the current one to improve decoding accuracy.

B. Decoding based on spatial attention

This study used modulated signals as the stimuli. We expected that attention would enhance the neural representation of the steady-state response of the modulation. Instead, the high feature weights in parietal alpha and temporal gamma indicated that spatial attention was the dominating factor of attention decoding in this study.

Steady-state responses played a less important role in this BCI design than in a typical ASSR/SSSEP-based BCI system. One explanation for such difference is the use of discrete stimuli. The pulses might have been processed by the brain as individual events instead of a continuous stream, so the brain never truly entered a steady state during the experiment. Using continuous stimuli, such as natural speech, might help enhance the representation of steady-state response in EEG.

C. Transfer learning

The cross-session validation results were comparable to their corresponding within-session results. It indicates that the participants might have adopted a similar strategy to focus even on different days. The modest drop in some participants might be due to a slightly different EEG cap placement between sessions. This result demonstrates some transfer learning ability in the proposed BCI system, showing potential in improving the model through multiple training sessions [20].

V. CONCLUSIONS

The current study proposed a new BCI system based on auditory and tactile attention. It yielded an efficiency comparable to or even higher than the existing BCI paradigms, without engaging the user's hands or eyes. The highest efficiency achieved in the tactile condition was close to a visual-based BCI. The system also demonstrated certain transfer learning ability.

REFERENCES

[1] R. Abiri, S. Borhani, E. W. Sellers, Y. Jiang, and X. Zhao, "A comprehensive review of EEG-based brain-computer interface paradigms," *Journal of Neural Engineering*, vol. 16, no. 1, p. 011001, 2019.

[2] Z. Lin, C. Zhang, Y. Zeng, L. Tong, and B. Yan, "A novel P300 BCI speller based on the Triple RSVP paradigm," *Scientific Reports*, vol. 8, p. 3350, dec 2018.

[3] J. Chen, D. Zhang, A. K. Engel, Q. Gong, and A. Maye, "Application of a single-flicker online SSVEP BCI for spatial navigation," *PLoS ONE*, vol. 12, p. e0178385, may 2017.

[4] F. Ferracuti, A. Freddi, S. Iarlori, S. Longhi, and P. Peretti, "Auditory paradigm for a P300 BCI system using spatial hearing," in *IEEE International Conference on Intelligent Robots and Systems*, pp. 871–876, 2013.

[5] S. Ahn, M. Ahn, H. Cho, and S. Chan Jun, "Achieving a hybrid brain-computer interface with tactile selective attention and motor imagery," *Journal of Neural Engineering*, vol. 11, no. 6, p. 066004, 2014.

[6] H. J. Baek, M. H. Chang, J. Heo, and K. S. Park, "Enhancing the Usability of Brain-Computer Interface Systems," *Computational Intelligence and Neuroscience*, vol. 2019, p. 5427154, 2019.

[7] M. Spüler and S. Kurek, "Alpha-band lateralization during auditory selective attention for brain-computer interface control," *Brain-Computer Interfaces*, vol. 5, pp. 23–29, jan 2018.

[8] Y. Deng, R. M. Reinhart, I. Choi, and B. G. Shinn-Cunningham, "Causal links between parietal alpha activity and spatial auditory attention," *eLife*, vol. 8, p. e51184, nov 2019.

[9] Y. Deng, I. Choi, and B. Shinn-Cunningham, "Topographic specificity of alpha power during auditory spatial attention," *NeuroImage*, vol. 207, p. 116360, feb 2020.

[10] W. W. An, K. H. Ting, I. P. Au, J. H. Zhang, Z. Y. Chan, I. S. Davis, W. K. So, R. H. Chan, and R. T. Cheung, "Neurophysiological Correlates of Gait Retraining with Real-Time Visual and Auditory Feedback," *IEEE Transactions on Neural Systems and Rehabilitation Engineering*, vol. 27, pp. 1341–1349, jun 2019.

[11] I. Choi, L. Wang, H. Bharadwaj, and B. Shinn-Cunningham, "Individual differences in attentional modulation of cortical responses correlate with selective attention performance," *Hearing Research*, vol. 314, pp. 10–19, 2014.

[12] A. Delorme and S. Makeig, "EEGLAB: an open source toolbox for analysis of single-trial EEG dynamics including independent component analysis," *Journal of Neuroscience Methods*, vol. 134, pp. 9–21, mar 2004.

[13] J. A. Palmer, K. Kreutz-Delgado, and S. Makeig, "Super-Gaussian Mixture Source Model for ICA," *Lecture Notes in Computer Science*, pp. 854–861, Springer Berlin Heidelberg, mar 2006.

[14] A. Mognon, J. Jovicich, L. Bruzzone, and M. Buiatti, "ADJUST: An automatic EEG artifact detector based on the joint use of spatial and temporal features," *Psychophysiology*, vol. 48, pp. 229–240, feb 2011.

[15] E. Combrisson and K. Jerbi, "Exceeding chance level by chance: The caveat of theoretical chance levels in brain signal classification and statistical assessment of decoding accuracy," *Journal of Neuroscience Methods*, vol. 250, pp. 126–136, jan 2015.

[16] H. J. Baek, H. S. Kim, J. Heo, Y. G. Lim, and K. S. Park, "Brain-computer interfaces using capacitive measurement of visual or auditory steady-state responses," *Journal of Neural Engineering*, vol. 10, p. 024001, apr 2013.

[17] M. Severens, J. Farquhar, J. Duysens, and P. Desain, "A multi-signature brain-computer interface: Use of transient and steady-state responses," *Journal of Neural Engineering*, vol. 10, no. 2, p. 026005, 2013.

[18] J. Li, J. Pu, H. Cui, X. Xie, S. Xu, T. Li, and Y. Hu, "An Online P300 BrainComputer Interface Based on Tactile Selective Attention of Somatosensory Electrical Stimulation," *Journal of Medical and Biological Engineering*, vol. 39, pp. 732–738, oct 2019.

[19] G. Townsend, B. K. LaPallo, C. B. Boulay, D. J. Krusienski, G. E. Frye, C. K. Hauser, N. E. Schwartz, T. M. Vaughan, J. R. Wolpaw, and E. W. Sellers, "A novel P300-based brain-computer interface stimulus presentation paradigm: moving beyond rows and columns," *Clinical neurophysiology*, vol. 121, pp. 1109–20, jul 2010.

[20] M. Wronkiewicz, E. Larson, and A. K. Lee, "Leveraging anatomical information to improve transfer learning in brain-computer interfaces," *Journal of Neural Engineering*, vol. 12, p. 046027, aug 2015.